Silicon (2021) 13:1285–1294
https://doi.org/10.1007/s12633-020-00662-4

ORIGINAL PAPER

Experimental Investigation and Analysis of Properties and Dry Sliding Wear Behavior of Al -Fe-Si Alloy Matrix Composites

S. Sakthivelu[1] · P. P. Sethusundaram[2] · M. Ravichandran[3] · M. Meignanamoorthy[3]

Received: 26 June 2020 / Accepted: 18 August 2020 / Published online: 23 August 2020

Abstract

Aluminium alloy finds widespread applications in numerous engineering industries because of its tremendous properties. However aluminium alloy possess poor wear resistance. This study aims to analyze the effect of Al_2O_3 reinforcement on the dry sliding performance of AA8011 matrix composites for braking applications. AA8011 matrix composite was produced via stir casting (SC) method. The various compositions are AA8011, AA8011- 4 wt.% Al_2O_3, AA8011–8wt. %Al_2O_3 and AA8011-12wt. %Al_2O_3. The Al_2O_3 particle distribution in the AA8011 matrix was studied via scanning electron microscopy (SEM). Hardness (H), tensile strength (TS) and compressive strength (CS) of the composites were studied. As of the study it has been found mechanical properties were higher on AA8011–8 wt.% Al_2O_3 composites. Hence AA8011–8wt. %Al_2O_3 composite was subjected to wear test at different process parameters load (P), disc velocity (V) and distance (D). The experiments were demonstrated via L9 orthogonal array. The results were optimized through Grey Relational Analysis (GRA). Optimum process parameters to attain the minimum wear rate and coefficient of friction (COF) was identified though the Grey relational analysis (GRA). 'P' was the utmost significant factor for the wear resistance and COF. Results showed that, the minimum wear and COF can be achieved for the P - 10 N, V - 3 m/s and D - 1500 m. From ANOVA, it has been found that load is the utmost noteworthy parameter (58.97%) impelling wear and COF.

Keywords AA8011 · Al_2O_3 · Stir casting · Grey relational analysis · ANOVA

1 Introduction

Composite materials are rapidly replacing the existing traditional engineering materials despite of its outstanding properties [1]. The properties of the materials may be custom-made via changing the weight percentage of reinforcements in matrix. Aluminium is one of the major material for the fabrication of metal matrix composites (MMC) despite of better strength, excellent wear resistance and good dimensional stability. AMC are being considered as important material in aerospace, military, naval and constructional applications. However many process were available for the fabrication of MMC, SC was found to be an economical and easier way for the production of aluminium matrix composites [2, 3]. Michael Rajan et al. [4] fabricated AA7075 reinforced with TiB_2 composites using SC technique. The investigation concluded that incorporation of TiB_2 particles improved mechanical properties of the MMC. Ali kankali et al. [5] synthesized Al7075/SiC composites by changing the weight percentage between 0 to 30% and reported that the mechanical properties were high on 10 wt% of SiC composites. Ul Haq M.I et al. [6] fabricated Al7075/Si_3N_4 MMC via SC to study the dry sliding wear and COF. He reported that Si_3N_4 particles improves the wear resistance and improved the mechanical properties. P. Anitha et al. [7] explored the wear behavior of Al7075 hybrid composite strengthened by alumina and graphite particles synthesized via SC. The results exposed that addition of reinforcements reduced the wear of composites significantly. Shivaprakash Y. M. et al. [8] analyzed the wear behavior of AA2024/fly ash particles. Wear and COF were reduced by adding the fly ash particles than base materials. K. Somasundara Vinoth et al. [9]

✉ S. Sakthivelu
sakthis1691@gmail.com

[1] Department of Mechanical Engineering, Mount Zion College of Engineering and Technology, Pudukkottai, Tamilnadu, India

[2] Department of Mechanical Engineering, M.Kumarasamy College of Engineering, Karur, Tamilnadu, India

[3] Department of Mechanical Engineering, K.Ramakrishnan College of Engineering, Trichy, Tamilnadu, India

synthesized AlSi10Mg/SiCp and optimized the dry sliding wear parameters using response surface genetic algorithm. Ghanaraja S et al. [10] analyzed the mechanical properties of hot extruded Aluminium/TiO_2 MMCs. It has been stated that extreme H and TS were achieved for 12 wt% TiO_2 reinforced with Al. H. Siddhi Jailaniet al [11] developed Al-Si (12 Wt.%) alloy–fly ash composites through powder metallurgy process and explored the wear behavior of composites. S. Gopalakrishnan et al. [12] fabricated AA6061 matrix composite strengthened with titanium carbide particles via SC route to improve the tribological properties of the matrix metal. The wear properties were analyzed through pin-on-disc apparatus. The results reported that specific strength and wear properties were enriched through the inclusion of TiC particles. B. Vijaya Ramnath et al. [13] produced and analyzed the mechanical properties of aluminium hybrid composite strengthened with Al_2O_3 and B_4C. The MMCs were synthesized through SC by varying the weight percentage of reinforcements. T. Rajmohan et al. [14] synthesized Al356 hybrid composites to examine the mechanical and wear behavior by adding SiC and mica particles via SC to increase the tribological properties of the composites. B. Ashok Kumar et al. [15] manufactured AA6061 composites reinforced with AlN particles through liquid metallurgy. The mechanical behaviour of the composites was studied and dispersion of particles was analyzed using optical and SEM images. P.B. Pawar et al. [16] et al. fabricated aluminium matrix composites strengthened with SiC particles using liquid metallurgy technique. Hardness test and SEM images were investigated in this work for spur gear applications. Abhishek Kumar et al. [17] synthesized aluminium 359 alloy AMCs were fabricated via electromagnetic SC process to control solidification rate. The composites were reinforced with alumina particles to explore the variation in mechanical properties by adding the reinforcement. Kenneth Kanayo Alaneme et al. [18] investigated the corrosion and tribological properties of Al-Si-Mg-rice husk ash and SiC particles composites. The composites were processed by SC by changing the weight percentage of reinforcements. S.A. Sajjadi et al. [19] fabricated A356 aluminium alloy strengthened with micro and nano alumina particles via liquid metallurgy route to study the H and CS. Dispersion of reinforcements were through SEM and optical microscopy. The result reveals that properties were enhanced by inclusion of reinforcement. K.Umanath et al. [20] examined the tribological behavior of Al6061 alloy strengthened with SiC and Al_2O_3 particles. The hybrid composites were synthesized via liquid metallurgy. M. Uthayakumar et al. [21] developed fly ash reinforced AA6351 AMCs through SC to analyze the tribological properties of the composites. The effects of parameters were optimized by GRA. K. Ravi Kumar et al. [22] synthesized the AA6063 strengthened with TiC particles via liquid metallurgy route to analyze the microstructure and mechanical behavior of composites. Kenneth Kanayo Alaneme et al. [23] examined the microstructure and mechanical properties of ground nut shell ash and SiC reinforced AMCs. The result reveals that the mechanical properties were enriched through incorporation of ground nut shell ash particles. K. Ravikumar et al. [24] fabricated AA 6082/TiC composites to analyze the mechanical properties. The MMC were synthesized via SC by changing the weight fraction of tungsten carbide particles. It has been concluded that the properties were improved initially and decreased later by adding the reinforcements. B. Praveen Kumar et al. [25] investigated the mechanical behaviour of Al-4.5%Cu alloy strengthened via bamboo leaf ash.

From the literature, this work involves to synthesize AA8011- Al_2O_3 composites and optimize the wear parameters for minimum wear and COF.

2 Experimental Details

In this research, AA8011 (Fe- 0.8, Si- 0.7, Cu-0.15, Mn- 0.15, Mg- 0.09, Zn- 0.25, Ti- 0.15 and Al- remaining) was reinforced with Al_2O_3 and synthesized through stir casting process. The experimental plan was represented in Fig. 1. The AA8011-Al_2O_3 composites were fabricated via SC route through changing the weight Al_2O_3 weight percentage. Al_2O_3 particles were weighed in electronic weighing machine and preheated in muffle furnace at 350 °C to improve the wettability of Al_2O_3 with AA8011. AA8011 was introduced into graphite crucible as billets and melted at 800 °C temperature. Vortex was formed in the molten slurry by mechanical stirring action. Warmed Al_2O_3 particles were acquaint with into the vortex which was produced by stirring action. The slurry was mixed simultaneously by the stirrer during the addition of Al_2O_3 particles for homogeneous distribution of Al_2O_3 particles in the melted AA8011 at 300 rpm for 15 min. Finally the stirred slurry were poured and casted into preheated rectangular mold in the dimension of 100 mm × 100 mm × 10 mm and in cylindrical mould having the dimension of 100 mm length and 20 mm diameter.

To analyze the dispersion of Al_2O_3 with the matrix, SEM images (VEGA3, TESCAN, Czech Republic) was used. The Rockwell Hardness (B scale) was used to measure the hardness by applying 100 Kgf load in three points on the specimen. The hardness of the sample was determined according to ASTM standard E18.

The tensile test was carried out via computerized UTM. The test samples were prepared according to ASTM E08–8 standard. The compressive test was carried out by using computerized UTM and the samples were prepared according to ASTM E9–09 standards.

Tribological behavior of the AA8011–8 wt.% Al_2O_3 composites were investigated through pin on disc device displayed in Fig. 1 (f). The samples were machined in to size of 32 mm length and 10 mm diameter pin as ASTM G-99 standard. EN – 31 hardened steel disc was used as counter facing surface

Fig. 1 Experimental Plan

with the diameter of 90 mm. P, V and D were preferred as process variables and their levels were detailed in Table 1. The experiments were done using L9 OA and the parameters were optimized via GRA.

3 Results and Discussion

3.1 SEM Analysis

SEM images of the AA8011, AA8011-4wt.%Al_2O_3, AA8011–8wt.%Al_2O_3 and AA8011-12wt.%Al_2O_3 composites were reported in Fig. 2 (a-d). Figure 2 (a) shows the no evidence for the occurrence of Al_2O_3 particles in the AA8011 matrix. Figure 2 (b - d) displays the occurrence of Al_2O_3 particles in the matrix AA8011. Figure 2 (b) and 2 (c) specifies that the Al_2O_3 particles were distributed evenly in the AA8011 matrix. From Fig. 2 (d), it can be found that the addition of 12% of Al_2O_3 will result in agglomeration of the particles which degrades the properties of the composites.

Table 1 Process parameters and their levels

Symbols	Parameters	Unit	L1	L2	L3
A	P	N	10	15	20
B	V	m/s	1	3	5
C	D	m	1000	1500	2000

3.2 Influence of Al_2O_3 on Mechanical Properties

Figure 3 displays the influence of Al_2O_3 particles on the hardness of the AA8011 composite. From Fig. 3, it was clear that hardness was improved by adding 4% (57 HRB) and 8% (62 HRB) of Al_2O_3 particles paralleled to the base metal (52 HRB). The reason behind the improvement of hardness in composites was generation of dislocations because of variance in thermal enlargement between AA8011 and Al_2O_3. [29]. However the hardness begins to reduce while adding 12% Al_2O_3 particles (54 HRB). The cause behind the reduction in hardness at 12% Al_2O_3 was poor dispersion of Al_2O_3 particles

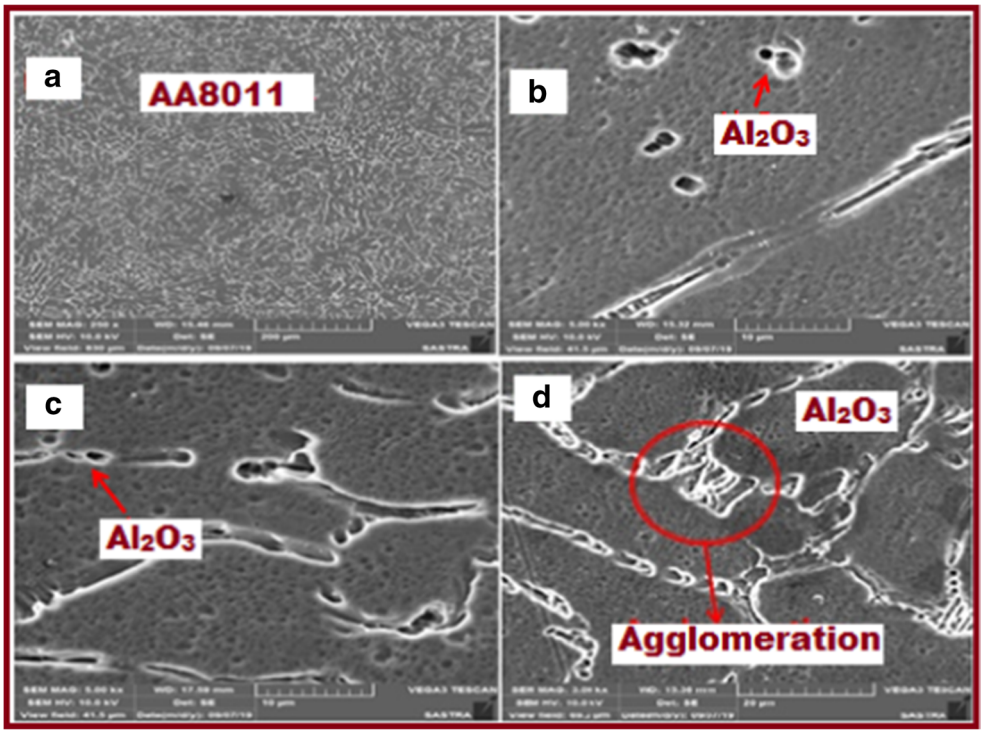

Fig. 2 (a) Pure AA8011, (b) AA 8011–4 wt.% of Al_2O_3 (c) AA 8011–8 wt.% Al_2O_3 and AA 8011–12 wt.% Al_2O_3

in AA8011. From Fig. 2 (d), the agglomeration of reinforcement can clearly identified, it could be understood that if the addition of Al_2O_3 particle exceeds 8% agglomeration could occur. It was evident that 8% Al_2O_3 composite has maximum hardness compared to other composites.

Figures 4 and 5 displays the TS and % elongation of the casted AA8011- Al_2O_3 composites. Figure 4 clearly depicts that the TS was improved gradually by the accumulation of Al_2O_3. The TS of all the composites was greater matched to the base matrix which proves that the incorporation of Al_2O_3 particles enhances the TS than the base metal with no substantial deprivation of % elongation to failure of the composites.

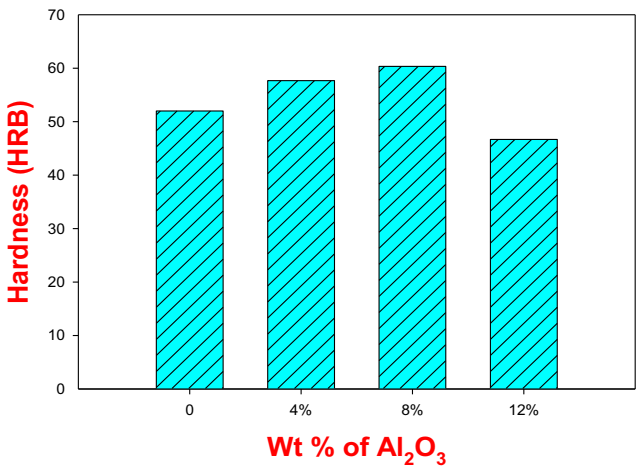

Fig. 3 Effect of Al_2O_3 on hardness

The TS was found to be maximum up to the addition of 8% of Al_2O_3. The increase in TS can be discussed based on load distribution to the reinforcement from matrix and the yield strength of the reinforcement particles. Yield strength of the material could be defined as role of reinforcement weight fraction via the subsequent expression.

$$\sigma_c = \sigma_m[W_r(1 + S/2) + (1-W_r)]$$

Where σ_c = composite yield strength, σ_m = matrix yield strength, W_r = weight fraction of reinforcement and s = aspect ratio of reinforcement particles. From the expression it could be understood that increasing the weight fraction of reinforcement improves the yield strength of the composites i.e. the capacity of the composites is maximum for with standing load

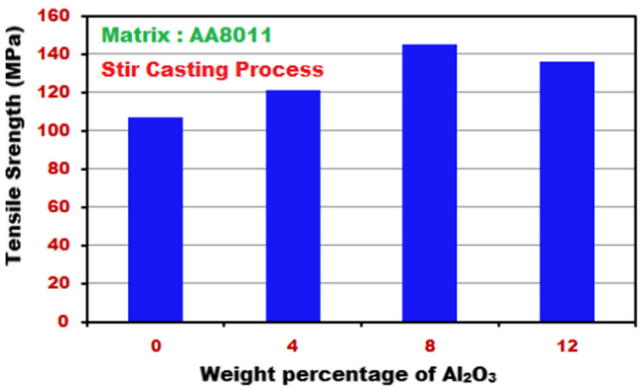

Fig. 4 Effect of Al_2O_3 on Tensile Strength

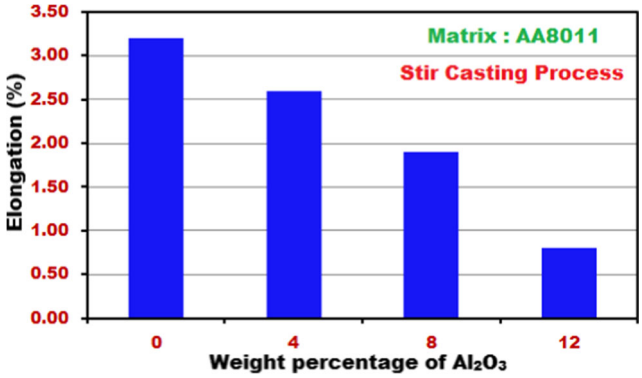

Fig. 5 Effect of Al_2O_3 on Percentage Elongation

[34]. However the inclusion of Al_2O_3 particles degrades the TS despite of poor distribution of the Al_2O_3 particles in the AA8011.

Figure 6 displays the CS of the AA8011- Al_2O_3 composites. It is evident that the CS improves gradually by expanding the weight percentage of Al_2O_3 particles than the matrix alloy. And also it can be observed that the CS related to TS increasing similarly respect to the homogeneous distribution of Al_2O_3 particles in AA8011 matrix. The occurrence of stiffer Al_2O_3 particles in the matrix AA8011 resist the wave of dislocations and plastic flow in the matrix which improves the CS of the composites [35]. But as in TS, the poor distribution of Al_2O_3 particles in matrix AA8011 degrades the CS after exceeding the incorporation of Al_2O_3 particles above 8%.

3.3 Wear and Frictional Analysis for AA 8011–8% of Al_2O_3 Composite

From the above results, AA 8011–8 wt.% Al_2O_3 composite displays superior mechanical properties H, TS and CS than AA 8011-4 wt.% of Al_2O_3 and AA8011-12 wt.% Al_2O_3 composite. Wear and frictional analysis were done to determine the better parameters to achieve least wear and COF of the composite using GRA. Trials were carried out as per L_9 OA as designed and experimental results were recorded in Table 2.

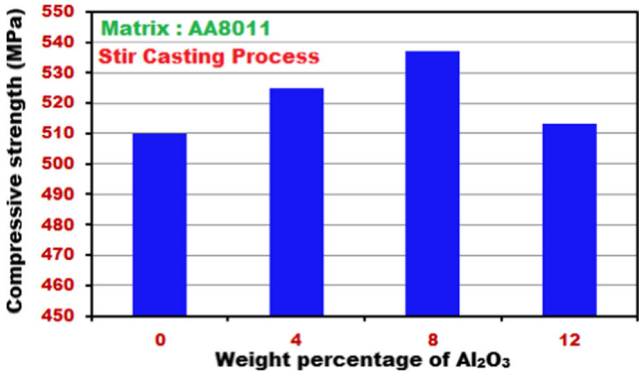

Fig. 6 Effect of Al_2O_3 on Compressive Strength

Table 2 Experimental results

Sl. No.	Load (N)	Disc velocity (m/s)	Sliding distance (m)	Wear rate (mm^3/m)	COF
1	10	1	1000	0.00482	0.312
2	10	3	1500	0.00397	0.264
3	10	5	2000	0.00381	0.281
4	15	1	1500	0.00248	0.326
5	15	3	2000	0.00454	0.287
6	15	5	1000	0.00668	0.364
7	20	1	2000	0.00507	0.442
8	20	3	1000	0.00696	0.371
9	20	5	1500	0.00742	0.351

3.3.1 Grey Relational Analysis

In two or more response problem, it is difficult to identify the optimum parameter for the responses. This situation is called as grey which means indeterminate information. So, a technique called as grey relational analysis is employed to analyze the complicated uncertainty with the help of grey relational grade. Scientist Deng proposed this theory in 1982. Grey relational analysis could be efficiently enforced to elucidate multi response problems. Initially the data is normalized in the range 0 and 1 [26].

In this work, the response values were wear rate and COF should be minimum. So the response values are normalized using "smaller the better quality" character by Eq. 1 and reported in Table 3.

$$y_i^*(x) = \frac{\max y_i(x) - y_i(x)}{\max y_i(x) - \min y_i(x)} \quad (1)$$

where m and n denotes the number of experimental data and responses. $y_i(x)$ designates the original sequence, $y_i^*(x)$ designates the arrangement subsequently the data preprocessing, max $y_i(x)$ exemplifies the extreme value of $y_i(x)$, min $y_i(x)$ exemplifies the least value of $y_i(x)$, and x is the required value. After the normalization, Grey relational coefficient ξ is calculated using Eq. 2 and recorded in Table 3.

$$\xi_i(K) = \frac{\Delta\min + p\Delta\max}{\Delta x_i(k) + p\Delta\max} \quad (2)$$

Finally, grey relation grade (GRG) was determined to change multi response problem into single response problem and GRG indicates the relationship between comparability and reference sequence [27]. GRG was calculated using Eq. 3 and ranked in order which is shown in Table 3.

$$\gamma_i = \frac{1}{n}\sum_{i=1}^{n}\xi_i(k) \quad (3)$$

Table 3 Grey Co-efficient and GRG

Exp No.	Normalized values		Deviation Sequence		Grey Co-efficient		GRG	Rank
	WR	COF	WR	COF	WR	COF		
1	0.526316	0.730337	0.473684	0.269663	0.513514	0.649635	0.582	5
2	0.698381	1	0.301619	0	0.623737	1	0.812	1
3	0.730769	0.904494	0.269231	0.095506	0.65	0.839623	0.745	3
4	1	0.651685	0	0.348315	1	0.589404	0.795	2
5	0.582996	0.870787	0.417004	0.129213	0.545254	0.794643	0.670	4
6	0.149798	0.438202	0.850202	0.561798	0.370315	0.470899	0.421	6
7	0.475709	0	0.524291	1	0.488142	0.333333	0.411	8
8	0.093117	0.398876	0.906883	0.601124	0.355396	0.454082	0.405	9
9	0	0.511236	1	0.488764	0.333333	0.505682	0.420	7

Where, γ_i is the necessary GRG for 'i'th experiment and n = number of response values. Figure 4 shows the interaction for GRG with load, disc velocity and sliding distance.

From GRG, influence of each parameter was calculated and presented in Table 4. The optimum parameter was chosen based on the higher mean values in response table for each parameter. From the Fig. 4, the optimum parameter chosen from the peak points for better wear resistance and minimum COF was A1-B2-C2 i.e. load 10 N, disc velocity of 3 m/s and sliding distance of 1500 m. From the rank in Table 4 and Fig. 7, it can be determined that load was the most inducing parameter trailed by sliding distance and velocity for minimum wear and COF.

Next optimal value of GRG for predicted parameters was calculated to identify the improvement by conducting confirmation experiments. The optimal value was predicted using the Eq. 4.

$$\gamma_e = \gamma_m + \sum_{i=1}^{r}(\gamma_i - \gamma_m) \quad (4)$$

where r denotes the total number of input process parameters, γ_i denotes the mean GRG value at the optimum level of 'i'th parameter and γ_m indicates total mean GRG. From Eq. 4, the optimal GRG for the predicted parameter was 0.8486.

Table 4 Response table for mean GRG

Parameters	Level1	Level 2	Level 3	Delta	Rank
Load	**0.7128***	0.6284	0.4117	0.3011	1
Disc velocity	0.5957	**0.6289***	0.5283	0.1005	3
Sliding distance	0.4690	**0.6754***	0.6085	0.2064	2

3.3.2 Analysis of Variance (ANOVA)

ANOVA was conducted at 95% confident level to find the major impact of parameters. ANOVA is also utilized to identify the percentage role of individual wear parameters which influences the response values [28]. ANOVA was performed for GRG and reported in Table 5. From Fig. 8, it can be noted that load was the dominating parameter to attain better wear resistance and minimum COF of the MMC with a contribution of 58.97% [30].

3.3.3 Impact of Process Parameters on Wear

Figure 9 (a- c) displays the contour plot for wear versus load, disc velocity and sliding distance to understand the dominating process parameter for least wear rate. Figure 9 (a) indicates the contour plot for the wear relating to load and disc velocity. From Fig. 9 (a), it can be understand that the wear rate was minimum (<0.003 mm^3/m) at lesser disc velocity (1 m/s) and

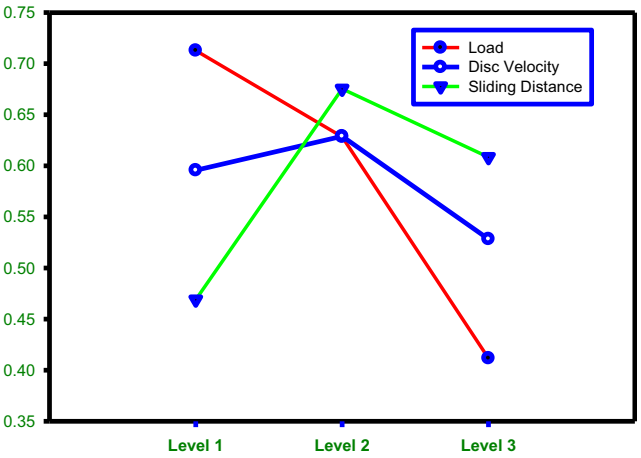

Fig. 7 Main effects plot for response table

Table 5 ANOVA

Source	DF	Adj SS	Adj MS	F-Value	Contribution (%)
Load	2	0.14475	0.072376	7.85	58.97
Disc velocity	2	0.01575	0.007874	0.85	6.42
Sliding distance	2	0.06653	0.033266	3.61	27.10
Error	8	0.01845	0.009225		7.52
Total	15	0.24548			100.00

load (10 N). By increasing the load and sliding distance the wear rate gradually increases. Figure 9 (b) displays the contour plot for load and sliding distance for the response wear rate. Fig. 9 (b) specifies that at nominal load (15 N) and disc velocity (3 m/s), the wear rate was lower (<0.003mm^3/m) compared to higher load and disc velocity. It also shows that the wear was larger at higher loads irrespective of sliding distance. Figure 9 (c) displays the plot for the response wear rate with respect to sliding distance and disc velocity. From Fig. 9 (c) it can be understand that the lesser wear (<0.003mm^3/m) occurs at lower disc velocity and sliding distance. This is despite of lesser contact time amid the disc and pin [32]. And also it is noted that larger wear (>0.007 mm^3/m) was observed by increasing the disc velocity.

3.3.4 Impact of Process Parameters on COF

Figure 10 (a-c) exemplifies the contour plot for COF with respect to load, disc velocity and sliding distance. Figure 10 (a) indicates the plot for COF with respect to load and disc velocity. From Fig. 10 (a), it can be observed lesser COF (<0.28) at minimum loading condition (10 N) and nominal disc velocity (3 m/s). And also it

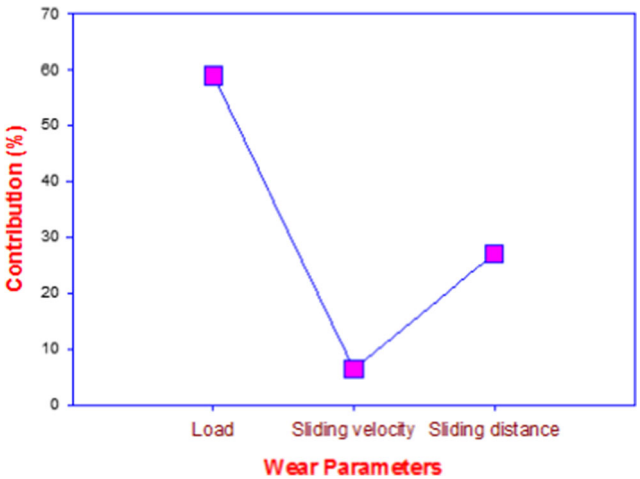

Fig. 8 Influence of wear parameters

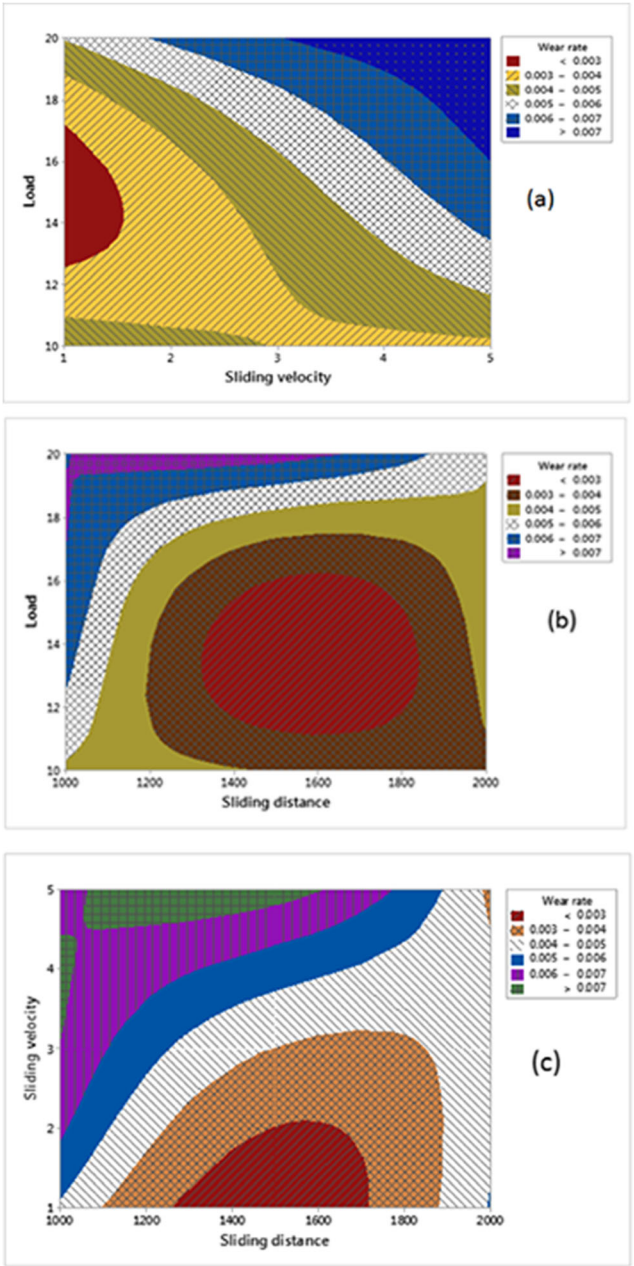

Fig. 9 Contour plot for wear rate

indicates higher wear rate (>0.4) by increasing the load even at lower disc velocity. Figure 10 (b) demonstrates the plot load vs. sliding distance for COF. Figure 10 (b) shows the minimum COF (<0.28) at lower load (10 N) and average sliding distance (1500 m). COF was maximum (>0.4) at higher by increasing the load and sliding distance. Figure 10 (c) displays the plot for COF relating to sliding distance and disc velocity. Figure 10 (c) indicates that the COF will be low (<0.28) at average disc velocity (3 m/s) and sliding distance (1500 m). However there was no any variation in COF by changing the sliding distance.

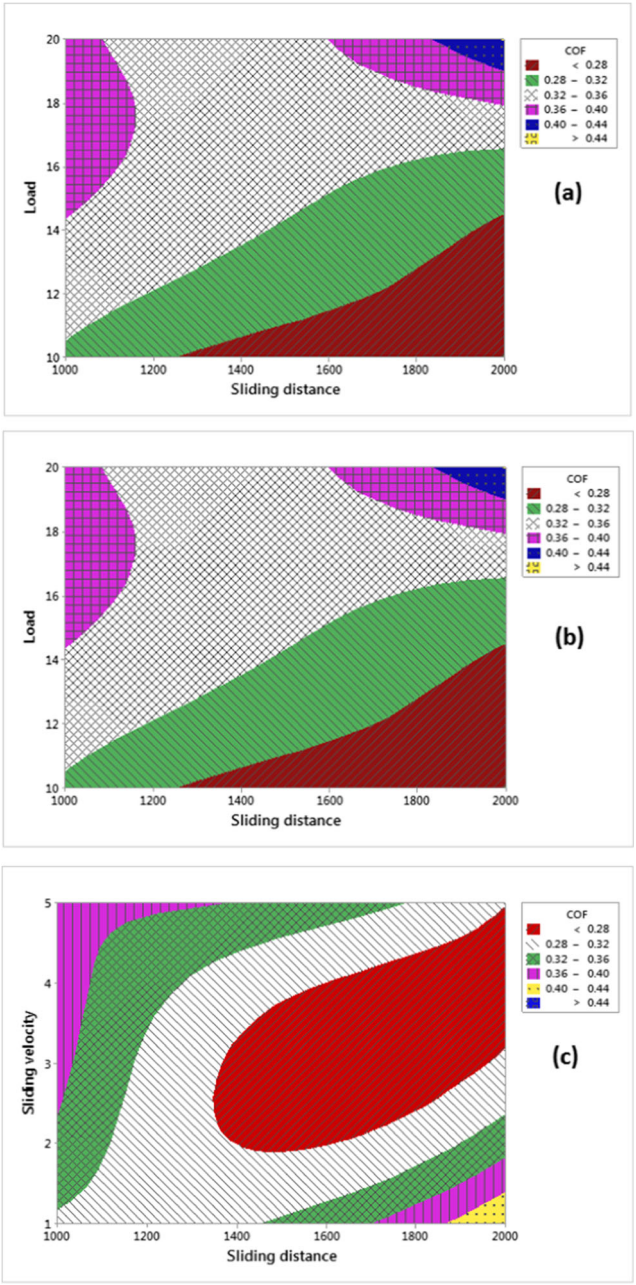

Fig. 10 Contour plot for COF

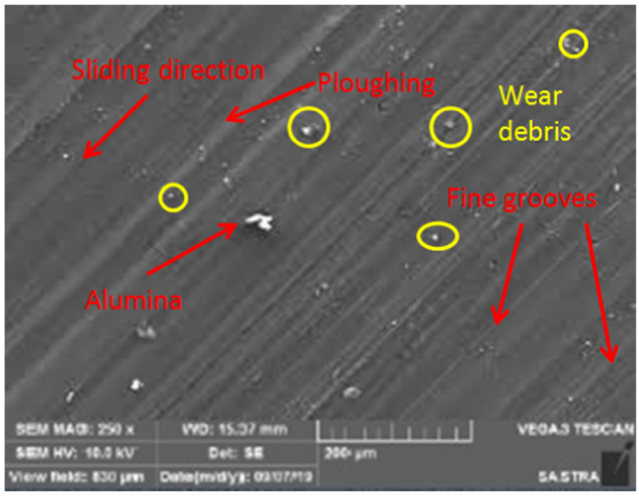

Fig. 11 Worn surface of AA8011–8wt.%Al_2O_3 at a load of 10kN, disc velocity of 3 m/s and sliding distance of 1500 m

3.4 Confirmation Test

Finally confirmation tests were carried out to check the enhancement in grade from initial setting to predicted parameter setting. The experiments were conducted and recorded in Table 6. GRG for predicted parameter was calculated to be 0.7841 using Eq. 4. The improvement of the grade from initial parameter setting to predicted parameter setting is 0.3794 i.e. 51% was improved through grey relational grade.

3.5 Worn Surface Morphology

SEM image of worn surface of AA8011–8wt.%Al_2O_3 composite was clearly displayed in Fig. 11. The SEM clearly displays the grooves, ploughing and debris resulting from plastic deformation. This decrease in rigorousness of the worn surface of the material was because of the formation of a thin film formation which inhibits the straight interaction of the sample with the rotating steel disc surface. Alumina was responsible for playing an operative part for possession the wear behavior of the AA8011–8wt.%Al_2O_3 composite was low.

As the load was applied over the pin, the AA8011–8wt.%Al_2O_3 composite pin begins to slide over the counter

Table 6 Confirmation Experiment

	Initial parameter Setting	Predicted	Optimal Parameter setting
Load	20	10	10
Disc velocity	3	3	3
Sliding distance	1000	1500	1500
Wear	0.00696		0.00405
Co-efficient of friction	0.371		0.268
Grey Relational Grade	0.4047	0.8486	0.7841
Improvement = 0.7841–0.4047 = 0.3794			

face disc and wear debris were formed which was shown in Fig. 11. These wear debris act as a third body abrasion and grooves were formed by ploughing action. At higher loads, more wear debris was formed due to dry sliding between metal to metal contacts which promotes large scale plastic deformation, so that large amount of material will be removed from the composite surface. This will result in higher wear and co-efficient friction which can be justified from Table 2. It has been proved that the result obtained from the grey relational analysis i.e. the load value should be low for minimum wear and COF.

By increasing the disc velocity, the travel time required to complete the sliding distance will be minimum, such that the generation of wear debris will be reduced. Due to generation of less debris, the wear rate of the composite was decreased by increasing the disc velocity. The plastic deformation was higher velocity due to increased separation between the composite pin and abrasive particles. This leads to less surface damages of the composites compared to lower disc velocity [31]. At lower disc velocity, the contact time between the composite and the disc was high, so that the contact temperature between the surfaces [33] of the composite and disc was increased which generates a tribo-layer between the surfaces. Due to generation of the tribo layer, the co-efficient of friction between the surfaces was reduced at lower disc velocity.

4 Conclusions

In this present investigation, the wear performance of the AA8011–8wt. %Al_2O_3 composite was analyzed through pin on disc apparatus. The subsequent conclusions have been drained.

- AA8011-Al_2O_3 composites were produced effectively through stir casting process.
- The dispersal of Al_2O_3 particles with the AA8011 was examined using Scanning Electron Microscopy.
- Mechanical properties of the composite was gradually enriched despite of incorporation of Al_2O_3 particles.
- Tribological behavior of the AA8011–8wt.%Al_2O_3 composite was analyzed through GRA and the optimum condition for better wear resistance and minimum COF was determined as load applied = 10 N, disc velocity = 3 m/s and sliding distance = 1500 m. From grey relational analysis, the results were improved (51%) from the initial setting condition.
- Influence of individual process parameters for minimum wear and COF were discussed and load applied plays the dominating role for the wear and COF.
- Results obtained from grey relational analysis were confirmed with ANOVA.
- Wear mechanism was studied through scanning electron microscope image of worn surface.
- In future work, the machinability characteristics of AA8011–8%Al_2O_3 composite will be studied for the production of desired final component through abrasive water jet machining process and the optimum parameter will be identified for minimum kerf angle and maximum material removal rate.

References

1. Aribo S, Fakorede A, Ige O, Olubambi P (2017) Erosion-corrosion behavior of aluminum alloy 6063 hybrid composite. Wear 376-377: 608–614
2. Zhou W, Xu ZM (1997) Casting of SiC reinforced metal matrix composites. J Mater Process Technol 63:358–363
3. Ceschini L, Minak G, Morri A (2006) Tensile and fatigue properties of the AA6061/20vol% Al_2O_3p and AA7005/10vol% Al_2O_3p composites. Compos Sci Technol 66(2):333–342
4. Michael Rajan HB, Ramabalan S, Dinaharan I, Vijay SJ (2014) Effect of TiB_2 content and temperature on sliding wear behavior of AA7075/TiB_2 in situ aluminum cast composite. Arch Civ Mech Eng 14(1):72–79
5. Kalkanlı A, Yılmaz S (2008) Synthesis and characterization of aluminum alloy 7075 reinforced with silicon carbide particulates. Mater Design 29(4):775–780
6. Ul Haq MI, Anand A (2018) Dry sliding friction and Wear behavior of AA7075-Si_3N_4 composite. Silicon-Neth 10:1819–1829
7. Anitha P, Shrinivas Balraj U (2017) Dry sliding Wear performance of Al/7075/Al_2O_3p/Grp hybrid metal matrix composites. Mater Today 4(2):3033–3042
8. Shivaprakash YM, Yadavalli B, Sreenivasa Prasad KV (2013) Comparative study of tribological characteristics of AA2024+ 10% fly ash composite in non-heat treated and heat treated conditions. Int J Res Technol 2(11):275–280
9. Somasundara VK, Subramanian R, Dharmalingam S, Anandavel B (2014) Optimization of dry sliding wear conditions for AlSi10Mg/SiC_p composites using response surface: genetic algorithm approach. Ind Lubr Tribol 66(5):593–600
10. Ghanaraja S, Ramanuja C, Ravikumar KS, Madhusudan BM (2015) Study on mechanical properties of hot extruded Al(mg)-TiO2 composites. Am J Mater Sci 5(3C):188–193
11. Siddhi Jailani H, Rajadurai A, Mohan B, Sornakumar T (2017) Sliding wear behaviour of Al-Si alloy–fly ash composites produced by powder metallurgy technique. Ind Lubr Tribol 69(2):241–247
12. Gopalakrishnan S, Murugan N (2012) Production and wear characterization of AA 6061 matrix titanium carbide particulate reinforced composite by enhanced stir casting method. Compos Part B-Eng 43(2):302–308
13. Vijaya Ramnath B, Elanchezhian C, Jaivignesh M, Rajesh S, Parswajinan C, Ghias ASA (2014) Evaluation of mechanical properties of aluminium alloy–alumina–boron carbide metal matrix composites. Mater Design 58:332–338
14. Rajmohan T, Palanikumar K, Ranganathan S (2013) Evaluation of mechanical and wear properties of hybrid aluminium matrix composites. T Nonferr Metal Soc 23:2509–2517
15. Ashok Kumar B, Murugan N (2012) Metallurgical and mechanical characterization of stir cast AA6061-T6–AlNp composite. Mater Design 40:52–58

16. Pawar PB, Utpat AA (2014) Development of Aluminium based silicon carbide particulate metal matrix composite for spur gear. Procedia Mater Sci 6:1150–1156
17. Kumar A, Lal S, Kumar S (2013) Fabrication and characterization of A359/Al_2O_3 metal matrix composite using electromagnetic stir casting method. J Mater Res Technol 2(3):250–254
18. Alaneme KK, Adewale TM, Olubambi PA (2014) Corrosion and wear behaviour of Al–mg–Si alloy matrix hybrid composites reinforced with rice husk ash and silicon carbide. J. Mater. Res. Technol 3(1):9–16
19. Sajjadi SA, Ezatpour HR, Beygi H (2011) Microstructure and mechanical properties of Al–Al2O3 micro and nano composites fabricated by stir casting. Mater Sci Eng A 528(29–30):8765–8771
20. Umanath K, Palanikumar K, Selvamani ST (2013) Analysis of dry sliding wear behaviour of Al6061/SiC/Al2O3 hybrid metal matrix composites. Compos Part B-Eng 53:159–168
21. Uthayakumar M, Thirumalai Kumaran S, Aravindan S (2013) Dry sliding friction and Wear studies of Fly ash reinforced AA-6351 metal matrix composites. Adv Tribol 2013:1–6. https://doi.org/10.1155/2013/365602
22. Ravi Kumar K, Kiran K, Sreebalaji VS (2017) Micro structural characteristics and mechanical behaviour of aluminium matrix composites reinforced with titanium carbide. J Alloys Compd 723(5):795–801
23. Alaneme KK, Bodunrin MO, Awe AA (2018) Microstructure, mechanical and fracture properties of groundnut shell ash and silicon carbide dispersion strengthened aluminium matrix composites. J King Saud Univ Sci 30(1):96–103
24. Ravikumar K, Kiran K, Sreebalaji VS (2017) Characterization of mechanical properties of aluminium/tungsten carbide composites. Measurement 102(1):142–149
25. Praveen Kumar B, Birru AK (2017) Microstructure and mechanical properties of aluminium metal matrix composites with addition of bamboo leaf ash by stir casting method. T Nonferr Metal Soc 27(12):2555–2572
26. Noorul Haq A, Marimuthu P, Jeyapaul R (2008) Multi response optimization of machining parameters of drilling Al/SiC metal matrix composite using grey relational analysis in the Taguchi method. Int J Adv Manuf Tech 37(3–4):250–255
27. Panda A, Sahoo AK, Rout AK (2016) Multi-attribute decision making parametric optimization and modeling in hard turning using ceramic insert through grey relational analysis: a case study. Decis Sci Lett 5:581–592
28. Datta S, Bandyopadhyay A, Pal PK (2008) Slag recycling in submerged arc welding and its influence on weld quality leading to parametric optimization. Int J Adv Manuf Tech 39(3–4):229–238
29. SV Alagarsamy and M Ravichandran (2019) Synthesis, microstructure and properties of TiO_2 reinforced AA7075 matrix composites via stir casting route. Mater. Res. Express, 6(8)
30. D Srinivasan, M Meignanamoorthy, M Ravichandran (2019) Optimization of process parameters of boron carbide filled Aluminium matrix composites using Grey Taguchi method Mater Res Express 6(7)
31. Dharmalingam S, Subramanian R, Kök M (2013) Optimization of abrasive wear performance in aluminium hybrid metal matrix composites using Taguchi - grey relational analysis. P I Mech Eng J-J Eng 227(7):749–760
32. Alagarsamy SV, Ravichandran M (2019) Investigations on tribological behaviour of AA7075-TiO_2 composites under dry sliding conditions. Ind Lubr Tribol 71:1064–1071. https://doi.org/10.1108/ILT-01-2019-0003
33. Saravanan C, Subramanian K, Anandakrishnan V, Sathish S (2018) Tribological behavior of AA7075-TiC composites by powder metallurgy. Ind Lubr Tribol 70(6):1066–1071
34. Pazhouhanfar Y, Eghbali B (2018) Microstructural characterization and mechanical properties of TiB2 reinforced Al6061 matrix composites produced using stir casting process. Mater Sci Eng A 710:172–180
35. Fenghong C, Chang C, Wang Z, Muthuramalingam T, Anbuchezhiyan G (2019) Effects of silicon carbide and tungsten carbide in Aluminium metal matrix composites. Silicon-Neth 11:2625–2632